

# Topological and Energetic Landscapes of a Binuclear Beryllium Complex: Identifying Non-Nuclear Attractors and Correlation-Driven Stability

D. K. Jha<sup>1</sup>

<sup>1</sup>Department of Chemistry, Lunglei Government College, Lunglei, Mizoram, India. PIN 796701

Publication Date: 2026/04/09

**Abstract:** The nature of metal-metal bonding in main-group elements remains a significant challenge for electronic structure theory. In this work, we present a comprehensive computational study of a binuclear beryllium complex,  $\text{Be}_2\text{C}_{12}\text{N}_2\text{H}_{14}$ , utilizing Density Functional Theory (DFT) and high-level DLPNO-CCSD(T) calculations. The complex features a remarkably short Be–Be bond of 1.884 Å. Natural Bond Orbital (NBO) and Energy Decomposition Analysis (EDA-NOCV) confirm a strong covalent  $\sigma$ -bond stabilized by significant electron correlation and electrostatic interactions. Topological analysis via the Quantum Theory of Atoms in Molecules (QTAIM) reveals the presence of non-nuclear attractors, characterizing a unique electron-trapping bonding environment. Time-Dependent DFT (TD-DFT) predicts an intense absorption peak at 399.8 nm, suggesting potential applications in optoelectronic materials.

**Keywords:** LOL, ELF, LED, EDA-NOCV, NBO, QTAIM, DFT, Be-Be Bond.

**How to Cite:** D. K. Jha (2026) Topological and Energetic Landscapes of a Binuclear Beryllium Complex: Identifying Non-Nuclear Attractors and Correlation-Driven Stability. *International Journal of Innovative Science and Research Technology*, 11(4), 61-65. <https://doi.org/10.38124/ijisrt/26apr179>

## I. INTRODUCTION

The chemistry of beryllium is characterized by high toxicity and unique bonding protocols dictated by its  $s^2p^0$  valence configuration. While beryllium usually forms electron-deficient compounds, the realization of stable Be–Be bonds has become a focal point in main-group chemistry.<sup>1-15</sup> Theoretical models suggest that such bonds can be stabilized through the use of bulky, electron-donating ligands that mitigate the high reactivity of the Be centres.<sup>2</sup> This study aims to provide a multi-dimensional analysis of a specific  $\text{Be}_2$  complex,  $\text{Be}_2\text{C}_{12}\text{N}_2\text{H}_{14}$ , bridging the gap between geometric structure, energy decomposition, and topological electron density analysis to clarify the nature of the Be–Be interaction.

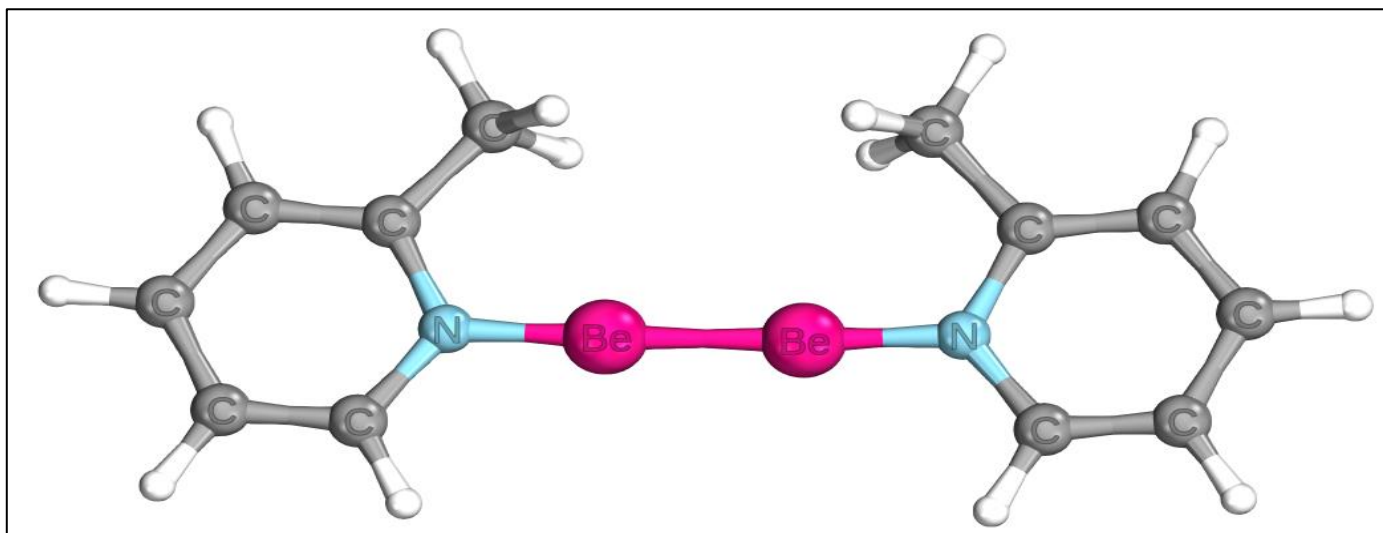
## II. COMPUTATIONAL METHODS

Geometry optimizations and vibrational frequency calculations were performed using the ORCA 6.0.1 package<sup>16</sup> at the TPSS/def2-TZVP level. Resolution of identity (RI) with the def2/J auxiliary basis was used for efficiency. Natural Bond Orbital (NBO) analysis, Energy Decomposition Analysis with Natural Orbitals for Chemical Valence (EDA-NOCV)<sup>18</sup> was performed to partition the binding energy. High-level correlation effects were evaluated using Local

Energy Decomposition (LED) at the DLPNO-CCSD(T) level.<sup>19</sup> Topological analyses, including QTAIM, Localized Orbital Locator (LOL), and Laplacian mapping, were performed using Multiwfn.<sup>20</sup>

## III. STRUCTURAL AND VIBRATIONAL RESULTS

The optimized structure of  $\text{Be}_2\text{C}_{12}\text{N}_2\text{H}_{14}$  shows a Be–Be bond length of 1.884 Å, significantly shorter than the sum of covalent radii. Coordination to the nitrogen atoms of the ligand occurs at 1.549 Å. Vibrational analysis confirmed the structure as a true minimum (zero imaginary frequencies). The Be–Be stretching vibration was identified at 579.27  $\text{cm}^{-1}$ , serving as a diagnostic IR signature for the metal-metal bond. Thermochemical analysis at 298.15 K yields a Gibbs free energy (G) of -604.8215 Eh, indicating high thermal stability.

Fig 1 Optimized Structure of  $\text{Be}_2\text{C}_{12}\text{N}_2\text{H}_{14}$ 

➤ *Natural Bond Orbital (NBO) and MO Analysis*

NBO analysis identifies a single  $\sigma$ -bond between Be10 and Be11 with a high occupancy of  $1.985 e^-$ . The hybrids are composed of 92% s-character and 7% p-character. Natural Population Analysis (NPA) assigns a partial charge of  $+0.59 e$  to the Be centres. Frontier molecular orbital analysis shows that the HOMO ( $-2.648 \text{ eV}$ ) is a bonding  $\sigma$ -orbital localized on the  $\text{Be}_2$  core (96% Be contribution), while the LUMO ( $-2.212 \text{ eV}$ ) is the corresponding antibonding  $\sigma^*$ -orbital.

➤ *Energy Decomposition (EDA-NOCV & LED)*

The bond energy was calculated at  $-73.18 \text{ kcal/mol}$  via EDA. The interaction is a balance between Electrostatic Attraction ( $-69.56 \text{ kcal/mol}$ ) and Orbital Interaction ( $-38.93$

$\text{kcal/mol}$ ), offset by Pauli Repulsion ( $+69.66 \text{ kcal/mol}$ ). NOCV analysis identifies the primary  $\sigma$ -donation ( $-17.21 \text{ kcal/mol}$ ) with density accumulation between the nuclei.<sup>21</sup>

The electronic structure of the central Be–Be unit can be described by the interaction of two sp-hybridized fragment orbitals. The EDA-NOCV Pair 0 corresponds to the formation of the  $\sigma$  Be–Be bonding orbital (HOMO). The large energy gap and the high occupancy ( $1.985e^-$ ) of this  $\sigma$  orbital, coupled with the empty  $\sigma^*$  orbital (LUMO), rationalize the short bond length of  $1.884 \text{ \AA}$ . This interaction is primarily s-s in nature (92% s-character per Be), which minimizes Pauli repulsion while maximizing the orbital overlap energy ( $\Delta E_{\text{orb}} = -38.93 \text{ kcal/mol}$ )

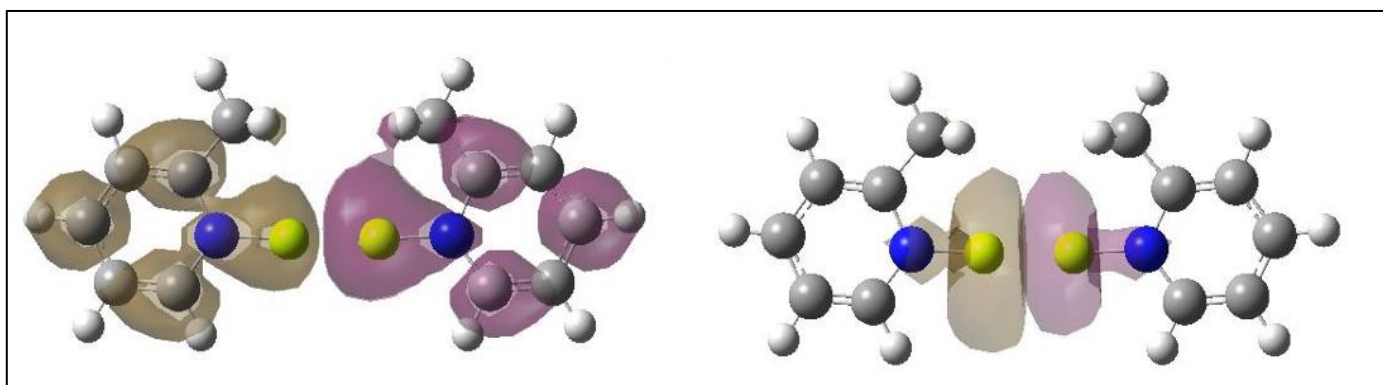


Fig 2 Plot of the deformation densities  $\Delta\rho_k$  for the two most significant NOCV pairs in the  $[\text{Be}_2\text{L}_2]$  complex. (Left) NOCV pair 0, representing the  $\sigma$  (Be–Be) bonding interaction ( $\Delta E = -17.21 \text{ kcal/mol}$ ). (Right) NOCV pair 1, representing ligand-to-metal coordination and  $\pi$ -reorganization ( $\Delta E = -2.16 \text{ kcal/mol}$ ). Red/Orange indicates density accumulation, while Blue indicates density depletion. Isosurface value =  $0.002 \text{ a.u.}$

The LED analysis at the DLPNO-CCSD(T) level provides a robust energetic benchmark for the Be–Be interaction.<sup>22-24</sup> The large inter-fragment correlation energy of  $-72.58 \text{ kcal/mol}$  highlights the 'charge-shift' nature of the bond, where correlation effects are as vital as the mean-field electrostatic terms. The orbital populations (Orbitals 52 and 53) show a near-equal distribution between both fragments (52%/48%), confirming a perfectly symmetric and highly covalent sharing of the bonding electrons within the  $\text{Be}_2$  core.

- Reference (HF) Interaction Energy ( $\Delta E_{\text{REF}}$ ):  $-854.68 \text{ kcal/mol}$
- Electrostatics ( $\Delta E_{\text{elstat}}$ ):  $-691.76 \text{ kcal/mol}$
- Exchange ( $\Delta E_{\text{exch}}$ ):  $-162.92 \text{ kcal/mol}$
- Total Inter-fragment Correlation:  $-72.58 \text{ kcal/mol}$ .
- Triples Correction [(T)]:  $-12.92 \text{ kcal/mol}$ .

➤ *Topological Analysis (QTAIM, LOL, Laplacian)*

Topological analysis confirms the Be–Be interaction via Bond Critical Points (BCPs) of type (3,-1). The Laplacian of electron density ( $\nabla^2\rho$ ) at the BCP is positive, while the Localized Orbital Locator (LOL) shows a localization plateau (>0.5) in the internuclear region.<sup>25-26</sup> Notably, the discovery of Non-Nuclear Attractors (NNAs) (Index 44, 67) suggests that electron density is trapped in the centre of the Be–Be bond, characteristic of metallic-like covalent bonding.

Localized orbital locator (LOL) map with superimposed bond paths and critical points. The high-value region between the Beryllium atoms indicates a formal bonding basin associated with the Be–Be  $\sigma$ -bond. Bond paths (solid lines) connect the (3,-3) nuclear/non-nuclear attractors through (3,-1) bond critical points.<sup>27-28</sup>

Table 1 Comprehensive Table of Topological Parameters

Interaction	Type	$\nabla^2\rho$ at BCP	Bonding Classification
Be–Be	(3,-1)	Positive (Depletion)	Charge-Shift / Metallic-like
Be–N	(3,-1)	Positive (Depletion)	Polar Covalent / Dative
C–C	(3,-1)	Negative (Concentration)	Shared Covalent

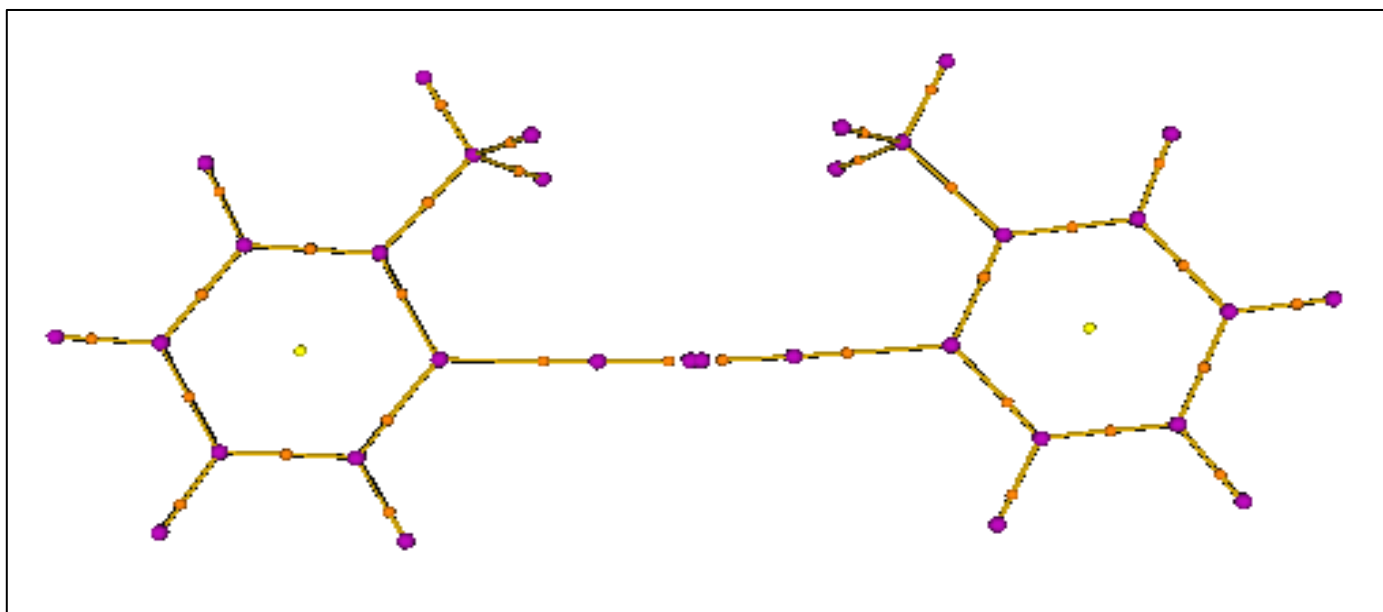


Fig 3 Molecular Graph (BCPs, RCPs, and Bond Paths)

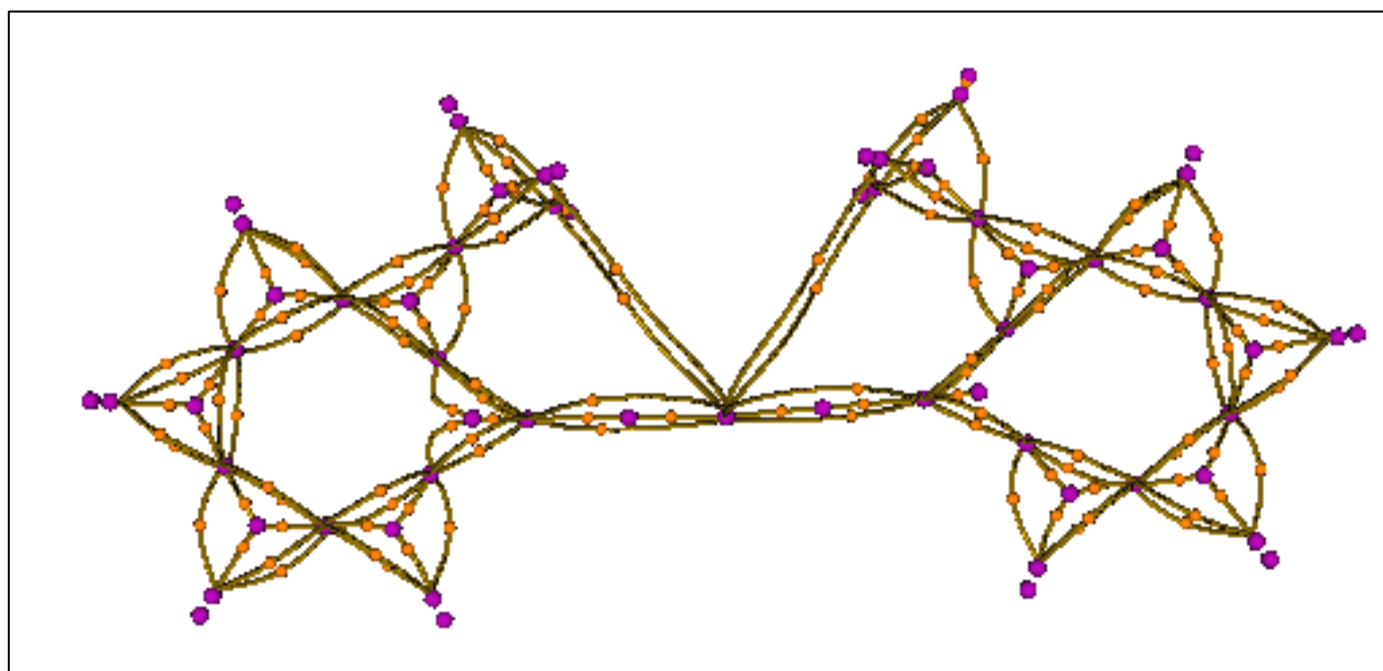


Fig 4 LOL Map with Bond Path Superposition

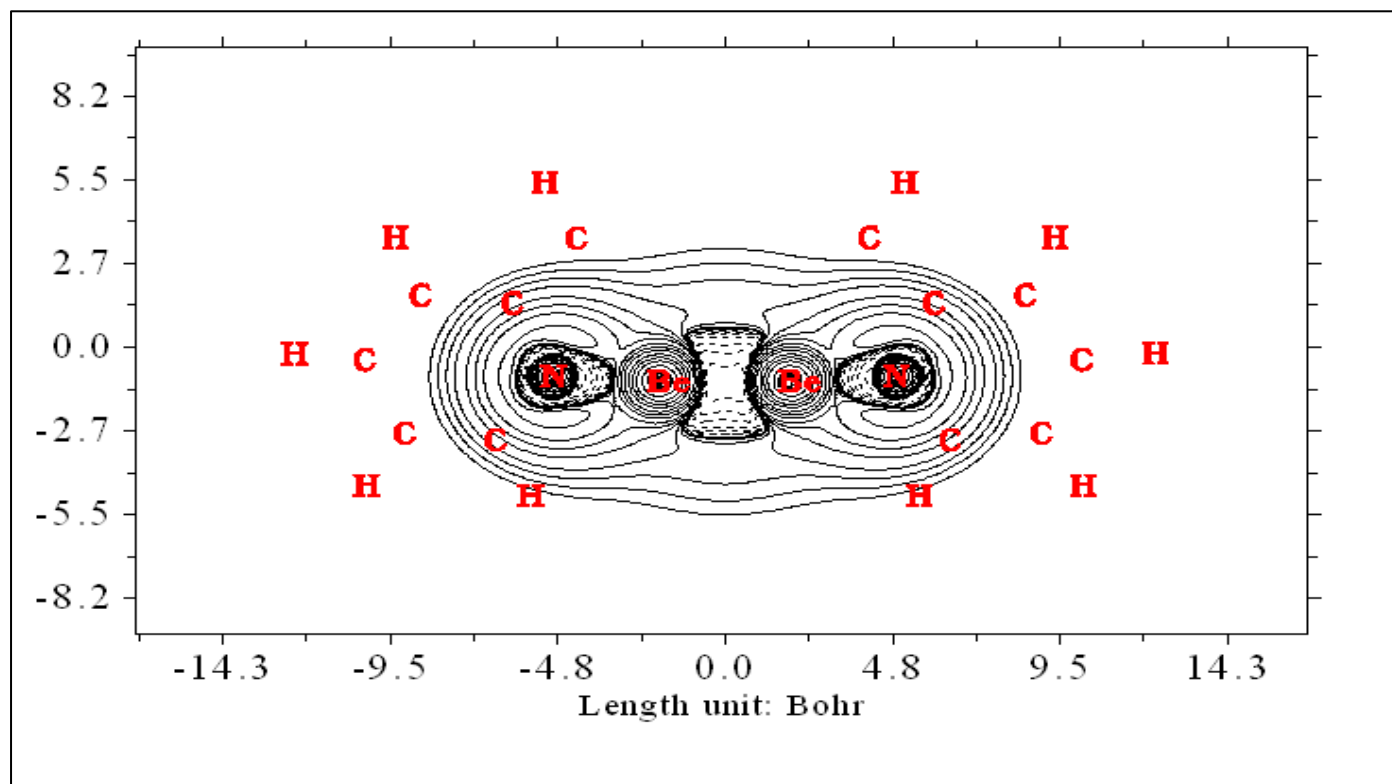


Fig 5 Contour map of the Laplacian of the electron density  $\nabla^2\rho$  in the Be–Be–N plane. Solid lines represent charge concentration ( $\nabla^2\rho < 0$ ) and dashed lines represent charge depletion ( $\nabla^2\rho > 0$ ). The bond paths and critical points are superimposed to illustrate the connection between the nuclear attractors and the bonding basins.

#### ➤ Electronic Spectra (TD-DFT)

TD-DFT calculations predict an intense ultraviolet absorption at 399.8 nm with an oscillator strength of  $f_{osc} = 3.86$ . This transition is identified as a Metal-to-Ligand Charge Transfer (MLCT) from the Be–Be bonding framework to the ligand  $\pi^*$ -orbitals. This high intensity suggests that the complex exhibits strong chromophoric properties.

#### IV. CONCLUSION

A robust, covalent Be characterizes the  $\text{Be}_2\text{C}_{12}\text{N}_2\text{H}_{14}$  complex–Be bond stabilized by both electrostatic and significant correlation effects. The unique topological signature of non-nuclear attractors and the intense 400 nm absorption peak distinguish this system as a significant example of main-group binuclear chemistry. This study provides a predictive framework for the experimental characterization of similar beryllium-based materials.

#### REFERENCES

- [1]. Frenking G, Herman HS (2007) The nature of the chemical bond in  $\text{Be}_2$ . *J Comput Chem* 28:73–86
- [2]. DK Jha, Beryllium-Trapped Electride Electrons: A Stable Non Nuclear Bridge in Triazole Dimers. *IJCRD* 2026; 8(3): 14-18. DOI: 10.33545/26646552.2026.v8.i3a.123
- [3]. DK Jha,  $\sigma$ -Aromatic Stabilization of a  $\text{Be}_4$  Core by NH Ligands: DFT Study, *IJCRD* 2026; 8(3): 06-13. DOI: 10.33545/26646552.2026.v8.i3a.122
- [4]. Z. H. Cui, W. S. Yang, L. Zhao, Y. H. Ding, G. Frenking (2016). *Angew. Chem. Int. Ed.*, 55, 7841; *Angew. Chem.* 2016, 128, 7972.
- [5]. Ariyaratna, I. R. and E. Miliordos (2020). "Be-Be Bond in Action: Lessons from the Beryllium-Ammonia Complexes  $[\text{Be}(\text{NH}(3))(0-4)](2)(0,2)$ ." *J Phys Chem A* 124(47): 9783-9792.
- [6]. Cong, F., et al. (2023). "Beryllium Dimer Reactions with Acetonitrile: Formation of Strong Be-Be Bonds." *Molecules* 29(1)
- [7]. Dong, X., et al. (2023). "B(7) Be(6) B(7) : A Boron-Beryllium Sandwich Complex." *Angew Chem Int Ed Engl* 62(31): e202304997. DOI/10.1002/anie.202304997
- [8]. Goesten, M. G. (2022). "Be-Be pi-Bonding and Predicted Superconductivity in  $\text{MBe}(2)$  ( $\text{M}=\text{Zr}, \text{Hf}$ )." *Angew Chem Int Ed Engl* 61(4): e202114303
- [9]. Michael C. Heaven, Vladimir E. Bondybey, Jeremy M. Merritt, Alexey L. Kaledin. (2011). "The unique bonding characteristics of beryllium and the Group IIA metals." *Chemical Physics Letters* 506(1-3): 1-14
- [10]. Michael C. Heaven, Jeremy M. Merritt, and Vladimir E. Bondybey. (2011). "Bonding in beryllium clusters." *Annu Rev Phys Chem* 62: 375-393.
- [11]. Mazumder, L. J. and A. K. Guha (2023). "Three-membered beryllium ring,  $\text{Be}(3)$ : not just a hydrogen bond acceptor." *Phys Chem Chem Phys* 25(31): 20947-20950
- [12]. Jeremy M Merritt, Vladimir E Bondybey, Michael C Heaven. (2009). "Beryllium dimer--caught in the act of bonding." *Science* 324(5934): 1548-1551.

- [13]. Shahnaz S Rohman, Chayanika Kashyap, Sabnam S Ullah, Ankur K Guha, Lakhya J Mazumder, Pankaz K Sharma. (2019). "Ultra-Weak Metal-Metal Bonding: Is There a Beryllium-Beryllium Triple Bond?" *Chem. Phys. Chem.* 20(4): 516-518
- [14]. Wen-Yan Tong, Tao-Tao Zhao, Xue-Feng Zhao, Xiaotai Wang, Yan-Bo Wu, Caixia Yuan. (2019). "Neutral nano-polygons with ultrashort Be-Be distances". *Dalton Trans* 48(42): 15802-15809.
- [15]. Eva Vos, Inés Corral, M. Merced Montero-Campillo, Otilia Mó, José Elguero, Ibon Alkorta and Manuel Yáñez. (2021). "Spontaneous bond dissociation cascades induced by Be(n) clusters (n = 2,4)". *Phys Chem Chem Phys* 23(11): 6448-6454
- [16]. Neese F (2022) The ORCA program system—Version 5.0. *WIREs Comput Mol Sci* 12:e1606
- [17]. Weinhold, F.; Landis, C. R. *Discovering Chemistry With Natural Bond Orbitals*, Wiley, 2012.
- [18]. Cárdenas Sabando, R.; Riplinger, C.; Wennmohs, F.; Neese, F.; Bistoni, G. Broadening the Scope of the ETS-NOCV scheme: A Versatile Implementation in ORCA, *J. Chem. Theory Comput.* 2025, doi.org/10.1021/acs.jctc.5c01003
- [19]. Bistoni G, et al. (2014) Local energy decomposition. *Angew Chem Int Ed* 53:12973-12977
- [20]. Lu T, Chen F (2012) Multiwfn: A multifunctional wavefunction analyzer. *J Comput Chem* 33:580-592
- [21]. Zhao Lili, Pan Sudip, Frenking Gernot (2022) *Comprehensive Computational Chemistry*
- [22]. Volume 2, 2024, Pages 322-361. Chapter: Energy Decomposition Analysis of the Chemical Bond: Scope and Limitation. DOI: 10.1016/B978-0-12-821978-2.00021-0.
- [23]. 9. Bistoni, G.; Riplinger, C.; Minenkov, Y.; Cavallo, L.; Neese, F. *Angew. Chem. Int. Ed.* 2014, 53, 12973-12977.
- [24]. A. Altun, I. F. Leach, F. Neese, G. Bistoni, *Angew. Chem. Int. Ed.* 2025, 64, e202421922. DOI: 10.1002/anie.202421922
- [25]. Cremer, D.; Kraka, E. Chemical bonds without bonding electron density—Does the difference electron-density analysis provide a solution to the problem? *Angew. Chem. Int. Ed. Engl.* 1984, 23, 627-628.
- [26]. Espinosa, E.; Molins, E.; Lecomte, C. Hydrogen bond strengths revealed by topological analyses of experimentally observed electron densities. *Chem. Phys. Lett.* 1998, 285, 170-173.
- [27]. Savin, A.; Nesper, R.; Wengert, S.; Fässler, T. F. ELF: The Electron Localization Function. *Angew. Chem. Int. Ed. Engl.* 1997, 36, 1808-1832.
- [28]. Schmider, H. L.; Becke, A. D. Chemical content of the kinetic energy density. *J. Mol. Struct. (Theochem)* 2000, 527, 51-61.